Journal of Atmospheric and Solar-Terrestrial Physics 72 (2010) 1212–1220

Contents lists available at ScienceDirect

Journal of Atmospheric and Solar-Terrestrial Physics

journal homepage: www.elsevier.com/locate/jastp

Simultaneous optical and radar measurements of meteors using the Poker Flat Incoherent Scatter Radar

R.G. Michell *

Southwest Research Institute, San Antonio, TX, United States

ARTICLE INFO

Article history:
Received 29 December 2009
Received in revised form
15 July 2010
Accepted 2 August 2010
Available online 6 August 2010

Keywords:
Incoherent scatter radar
Meteors
Optical meteors
Imaging
PFISR

ABSTRACT

Coordinated Poker Flat Incoherent Scatter Radar (PFISR) and imaging observations are examined in order to study the radar scattering signatures of optically visible meteors. Preliminary observations in 2006 revealed that optical meteors were detected by PFISR. A recent campaign in the winter of 2009, employed a radar mode optimized for meteor Doppler shifts. This paper presents a case study from 21 January 2009. Seven out of the 338 meteors observed with PFISR were also detected optically. Six out of those seven were detected by the side lobes of the radar and not the main beam. A positive correlation was found between the corrected backscattered radar power and the optical brightness of the meteors, as well as between optical brightness and absolute speed. Meteors originating in the east had higher speeds and more glancing incidence angles, while meteors originating in the north had lower speeds and more direct incidence angles.

1. Introduction and background

Meteors have been observed with radars since the 1940s (Appleton and Naismith, 1947; Lovell and Clegg, 1948) and the first television observations were carried out in the 1970s (Bakharev et al., 1977). The first comparisons of optical brightness to radar scattering properties of the ionized trail were done in the early 1980s (Znojil et al., 1980; Hapgood and Rothwell, 1982), but during the last decade, there have been many studies examining the physics of meteor ablation with observations, theory and modeling (McNeil, 1999; Oppenheim et al., 2000; Dyrud et al., 2002; Close et al., 2002; Oppenheim et al., 2003; Close et al., 2005; Dyrud et al., 2007; Dyrud and Janches, 2008). Different types of instrumentation have been used but, typically, each study focused on a single observational technique, such as radars (Reddi and Nair, 1998; Janches et al., 2003), lidars (Grime et al., 1999; Von Zahn, 2001), and optical means (spectroscopy and imaging) (Von Zahn, 1999; Clemesha et al., 2001; Shamir, 2005; Kaiser et al., 2004). There are, however, disproportionately less studies that combine multiple observational techniques. The combining of radar measurements and optical observations has been used in the past in order to gain insight into meteor ablation physics (Mathews et al., 2010; Brosch et al., 2004; Fujiwara et al., 1995; Pellinen-Wannberg et al., 1998; Szasz et al., 2008). Such a specific comparison has not yet been done with the Poker Flat Incoherent Scatter Radar (PFISR). It is therefore the purpose of this paper to specifically combine high-resolution optical imaging data with simultaneous PFISR measurements of head echoes, in order to examine the radar scattering signatures of visible meteors. Understanding this relationship will improve the accuracy of the many meteor studies that rely on radar data alone.

This study was motivated by data collected during an optical observational campaign coordinated with the preliminary engineering tests of the first quarter installation of PFISR during February and March of 2006. This test constituted the first scientific study using raw data from PFISR combined with high resolution imaging. Based on Advanced Modular Incoherent Scatter Radar (AMISR) technology, PFISR is constructed from a number of individual panels. At that time, PFISR contained only 32 panels, (one fourth of the final 128 panel configuration), in fact only 15 were operating. It was running at 449 MHz with four beam positions, one up the magnetic zenith (204.5° az., 77.8° el.), one up the true zenith (0° az., 90° el.) and the other two beams in between (209.1° az., 81.7° el.), (195.0° az., 86.0° el.), forming a fan shaped pattern. The radar mode consisted of long pulses (450 μs) with the raw voltage samples recorded at a cadence of ~30 ms, which enabled the observation of coherent meteor returns. It was optimized for ion line science and therefore had only 30 kHz of bandwidth, not enough to capture the high Doppler shifts associated with meteor head echoes. The receiver channel was actually set to filter out high Doppler shift returns. Given the small receiver bandwidth and bandpass, meteor head echoes had not been expected. This mode will hereafter be referred to as the "ion line mode".

* Tel.: +1 210 522 2279.
E-mail address: rmichell@swri.edu

1364-6826/$ - see front matter © 2010 Elsevier Ltd. All rights reserved.
doi:10.1016/j.jastp.2010.08.001

Table 1
Date and time, in UT, of the meteor observations along with the number of radar beams that the meteor passed through and whether radar backscatter was observed.

Meteor	Date	Time (UT)	# of beams	Scattering
1	24 February 2006	11:25:58	1	Yes
2	28 February 2006	12:23:54	1	No
3	28 February 2006	12:42:54	2	Yes
4	01 March 2006	09:20:42	2	Yes
5	01 March 2006	10:53:01	1	Yes
6	01 March 2006	10:56:39	1	Weak
7	01 March 2006	12:57:00	1	Weak
8	01 March 2006	13:01:19	1	No
9	01 March 2006	14:56:43	1	Yes

The imager used had a narrow FOV ($12^\circ \times 16^\circ$), which was centered on the magnetic zenith and recorded at 30 frames per second (fps). Optically, a total of nine meteors were observed to pass through the radar beam FOV locations, mapped to 100 km altitude. Of these nine, five produced strong radar backscatter, two did not show any sign of backscatter, and two showed weak signals in the radar data. The information regarding these nine meteors is summarized in Table 1, which presents the date, time, number of radar beams the meteor was observed to pass through and whether the radar scattering was observed.

Fig. 1 shows the optical and radar data from one of the brighter meteors identified in both PFISR and imager data. It is meteor # 9 on Table 1 and occurred on 01 March 2006 at 14:56:43 UT. The narrowfield image (left) is mapped to geodetic latitude and longitude with north up and east to the right. The white box represents the full-width-half-max (FWHM) radar beam FOV ($2^\circ \times 4^\circ$), mapped to 100 km altitude. The raw PFISR data (right) show the received power over a two second period. The meteor occurs at 43.4 s, where the strong backscatter only occurs at the beginning and end of the 67 km long pulse. These results motivated a higher bandwidth mode in the 2009 campaign.

The 2006 preliminary study revealed that most of the optical meteors were also detected by PFISR. This paper investigates in detail a case study from the night of 21 January 2009, where PFISR was running at full power (all 128 panels) in a mode optimized to capture the large positive Doppler shifts associated with meteors.

2. Observations

The night of 21 January 2009 had clear skies and narrowfield video data were recorded the entire night, providing a good case study to investigate the potential connection between optical and radar meteors. PFISR was running a raw data mode (hereafter referred to as the "meteor mode") with a long pulse (480 μs), sampled to 250 kHz of bandwidth, centered on +100 kHz, with five beam positions, in (205.7° az., 77.5° el.), and near the magnetic zenith (205.7° az., 74.5° el.), (205.7° az., 80.5° el.), (223.5° az., 77.35° el.), (195.0° az., 76.0° el.). During this night, the meteor mode encompassed four hours in the late evening/dawn sector, 2:37–6:30 LT (11:37–15:30 UT). The narrowfield imager used was the same as in the 2006 study ($12^\circ \times 16^\circ$ FOV, 30 fps).

It can be seen from Table 2 that the ion line mode should not observe meteors because the receiver bandpass is too small to detect their highly Doppler shifted returns. However, Fig. 1 does show that PFISR did detect a meteor, although it was only detected at the leading and trailing edges of the pulse. The net effect of the pulse edges interacting with the meteor Doppler bandwidth produced some backscattered power that was within the bandpass of the receiver. In reality, there would have been strong backscattered power throughout the altitude range (60–130 km) that corresponds to the pulse length, only they were at a Doppler shift that was larger than the receiver bandpass. The other meteors mentioned in Table 1, that showed signs of radar backscatter, also produced backscattered power only at the leading and trailing edges of the radar pulses.

Hereafter, all data presented and the resulting discussion refer to PFISR observations taken with the meteor mode, unless specifically noted otherwise.

The meteor mode is not optimal for resolving altitude propagation of meteors, due to the long uncoded pulse (480 μs) and long inter-pulse period (IPP) of 45 ms. The reason for this is because the meteor mode was a "piggy-back" mode on top of a mode that was optimized for doing ion line science, where reasonable spectral information of the returns was needed in multiple beam positions. Typical pulse lengths for PFISR meteor studies are 90 μs (Chau et al., 2009; Sparks et al., 2009). For a fully sampled point target, the range resolution is determined by the sampling frequency and not the pulse length, for example

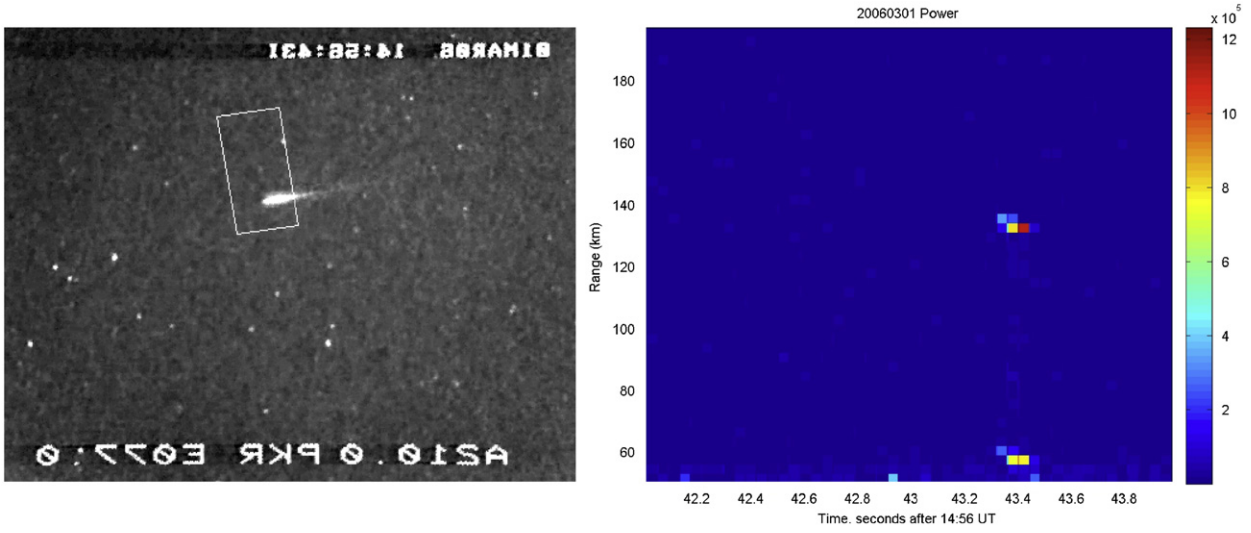

Fig. 1. Optical and radar data of the first meteor observed in both optical and PFISR data. The narrowfield image, on the left, shows the meteor passing through the radar beam location, mapped to 100 km, indicated by the white box. North is up and east is to the right in this view. The PFISR data, on the right, show the raw returned power for 2 s, revealing the meteor backscatter at 43.4 s.

Table 2
Summary of the radar mode characteristics for the two different modes discussed.

Radar mode	Ion line	Meteor
Transmit frequency (MHz)	449.3	449.3
Receiver frequency (MHz)	449.3	449.4
Pulse width (μs) (km)	450 [67]	480 [72]
Pulse coding	None	None
Inter-pulse period (ms)	40	45
Sampling frequency (kHz)	33.3	250
Receiver bandwidth (km/s)	−9 to +9	−83 to +150

Positive velocity is downward.

Mathews et al. (2008) have demonstrated a range resolution down to 150 m with PFISR.

Fig. 2 shows the radar and optical data for two of the seven meteors observed with the meteor mode on 21 January 2009. The data are presented in a similar format to Fig. 1, where the image data are on the left and the radar data are on right. This shows the better detection efficiency of the meteor mode over the ion line mode, as expected, with the returns spread in altitude over the length of the pulse. These two examples were chosen because they illustrate the concept of side lobe detection. The top row shows a fairly bright meteor passing far away from the main radar beam, yet still producing enhanced backscattered radar power. The bottom row shows a faint meteor that passes directly through the main beam, producing strong backscatter. The location of the meteor in the lower-left image is denoted by the white arrow, and was moving approximately from lower-right to upper-left. This clearly shows the connection between the optical meteors and the radar backscatter. In addition, the smaller meteor detected in the main beam, produced backscatter that was larger by more than a factor of 2. The other five meteors examined here exhibited similar relationships between the optical and radar data.

The first step in comparing the optical and radar data is to identify the times with enhanced backscatter in the radar data. These occur in the altitude range of approximately 60–130 km, consistent with meteor backscatter. This is done with a searching algorithm that identifies when the power, in this altitude range, is greater than a specified number of standard deviations (2.5 in this case) away from the mean. The data are visually inspected to remove the events that are not consistent with meteors, such as satellites and other noise signals. Fig. 3 shows an example output for the magnetic zenith position, covering 11:37–15:30 UT on 21 January 2009. A range of altitudes and intensities of meteor returns can be seen in this four hour period. Taking a fast Fourier transform (FFT) of these data reveals the line-of-sight (LOS) Doppler velocity of each meteor, shown in Fig. 4. The time index stated for the *x*-axes of Figs. 3 and 4 does not represent real time, as it is made up of many discontinuous short segments of radar data (only those with greatly enhanced power). This presentation

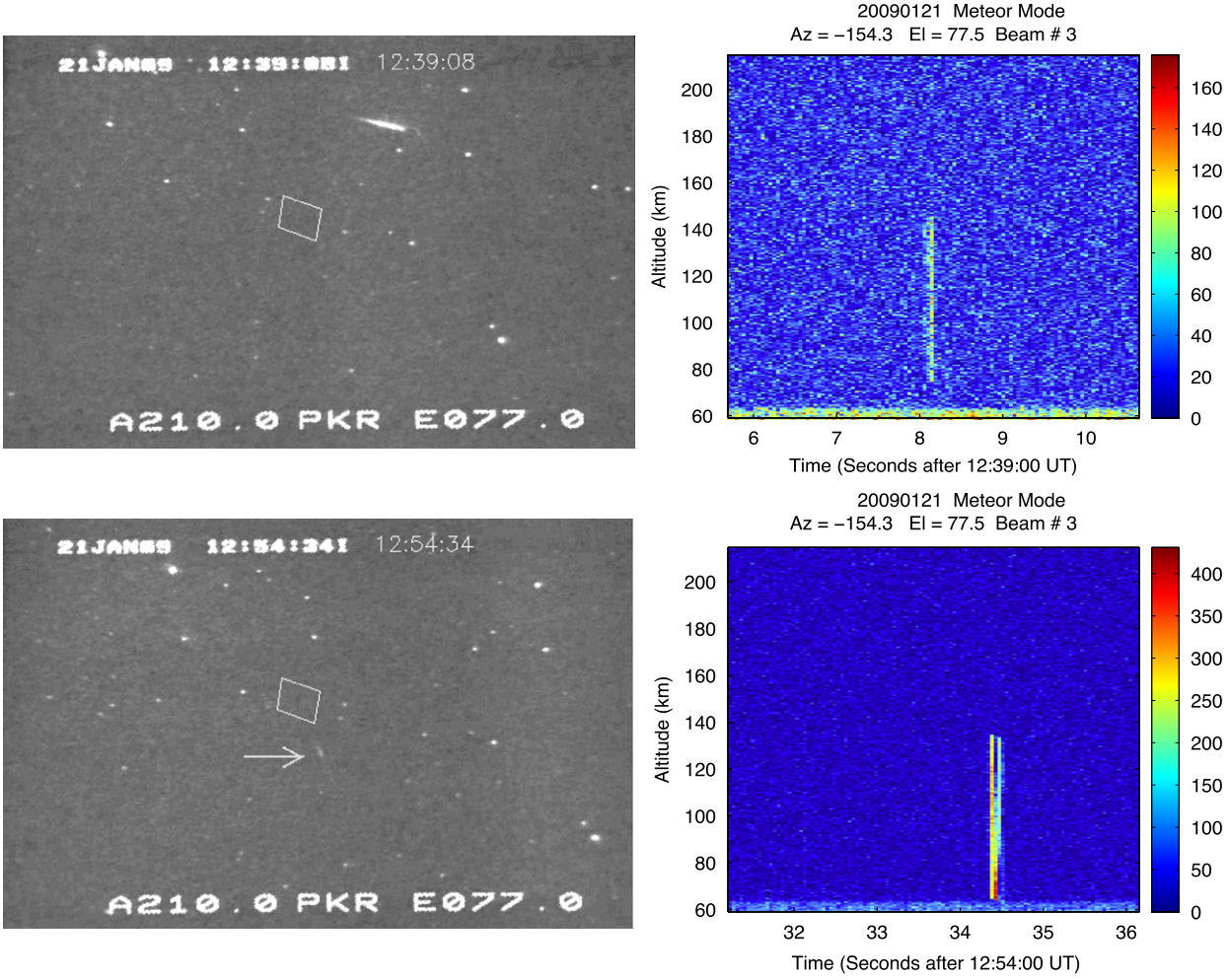

Fig. 2. Optical and radar data for two meteors observed in both optical and PFISR data. The narrowfield images, on the left, show the meteor locations relative to the main radar beam position, mapped to 100 km altitude, indicated by the white box. North is up and east is to the left in this view. The meteor in the lower left image is denoted by the white arrow and was moving in the lower-right to upper-left direction.

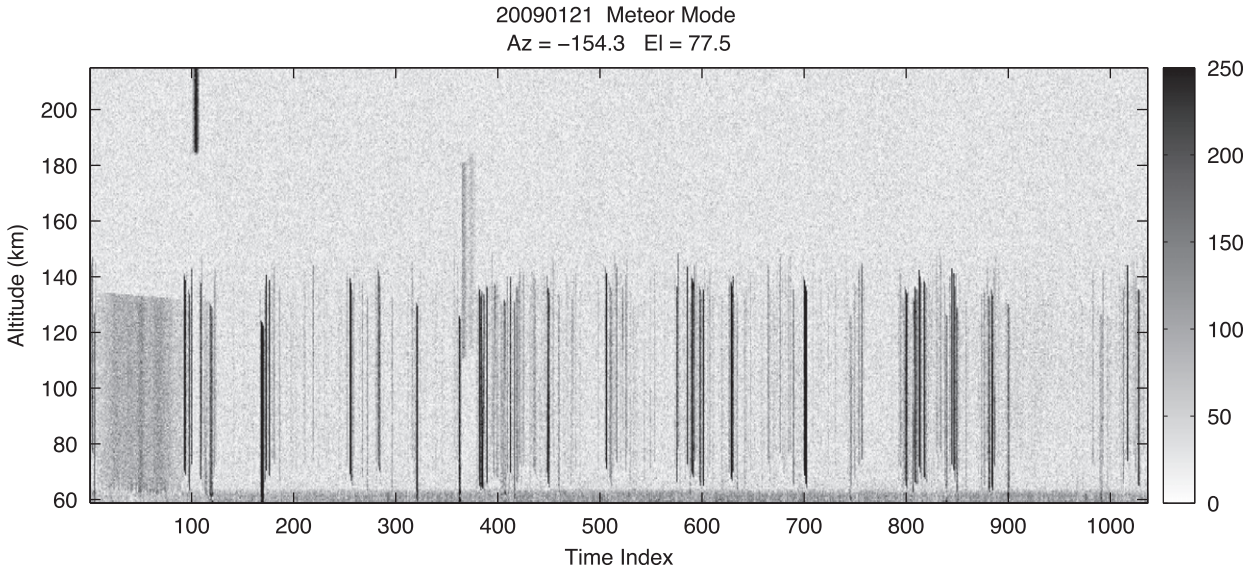

Fig. 3. Example output of the meteor searching algorithm for the magnetic zenith beam position of the meteor mode, covering 11:37–15:30 UT on 21 January 2009. This shows the raw returned power at the times with large backscatter in the altitude range of 60–220 km. The *x*-axis is the index of the return, from which the actual time in UT can be determined.

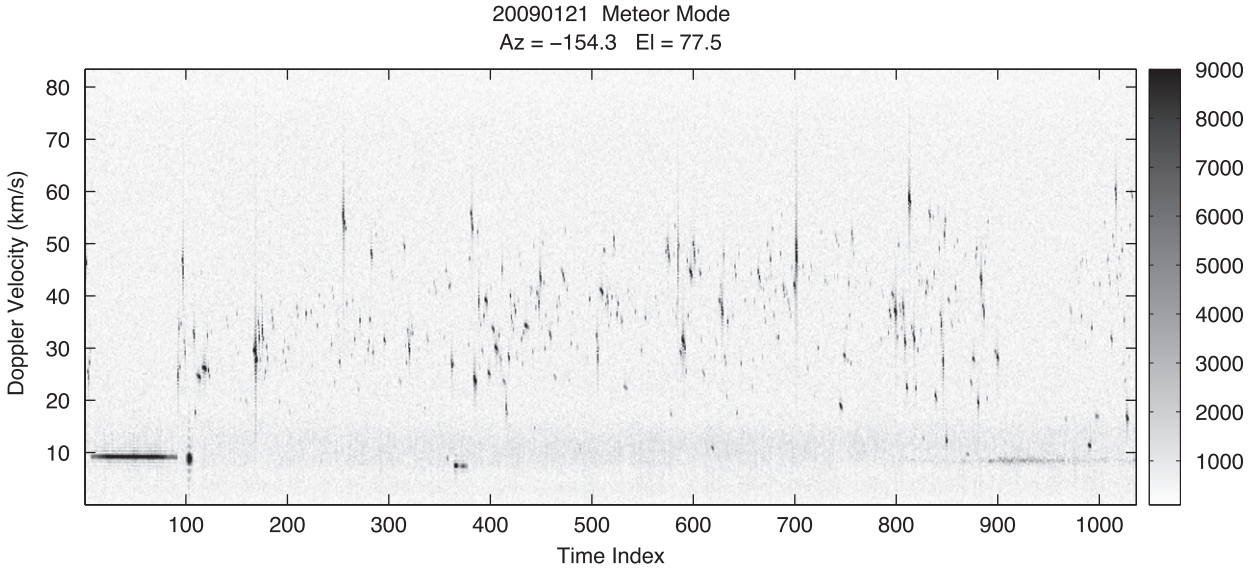

Fig. 4. FFT of the data in Fig. 3, showing the Doppler velocities of the meteors (and noise signals).

is meant to demonstrate the output and effectiveness of the searching algorithm.

An alternative searching approach, described in Sparks et al. (2009), is to identify peaks of large power in the FFT spectrum of the raw voltage samples and not within the backscattered power itself. An advantage of searching the FFT is that it provides an extra criteria for eliminating non-meteor returns from the results. The analysis presented here, searched the raw returned power levels and therefore needed an extra step to remove the non-meteor returns from satellites or space debris. It was done in this way to best compare to the optical images, by examining all the enhanced power returns that could potentially be from meteors, and then comparing to the imager data. One advantage of this method is a reduction in processing time because the FFT only needs to be computed for the output of the algorithm, a much reduced amount of data. In addition, several other sophisticated and robust searching algorithms are described in the literature, including Mathews et al. (2003) and Briczinski et al. (2009).

From the data contained in Figs. 3 and 4 the returned radar power and the LOS velocities can be quantified for each meteor. Fig. 5 is a scatter plot of the returned radar power versus LOS velocity for every meteor observed with the radar. The black dots show the meteors detected in the radar data alone, while the red stars show the meteors visible in both the radar and imager data. There is no clear correlation between LOS velocity and received radar power, although the highest power returns do occur at the higher LOS velocities.

It is known that radars detect meteors in their side lobes as well as the main beam, due to the large power of coherent returns (Dyrud and Janches, 2008; Chau et al., 2009). Therefore, it is a major advantage to have the optical data of these meteors because then their location relative to the main beam of the radar is known. For these seven optical meteors, only one of them passed directly through the main beam, while the other six passed through side lobes, thus resulting in a smaller apparent back-scattered radar power. The radar power was corrected using the

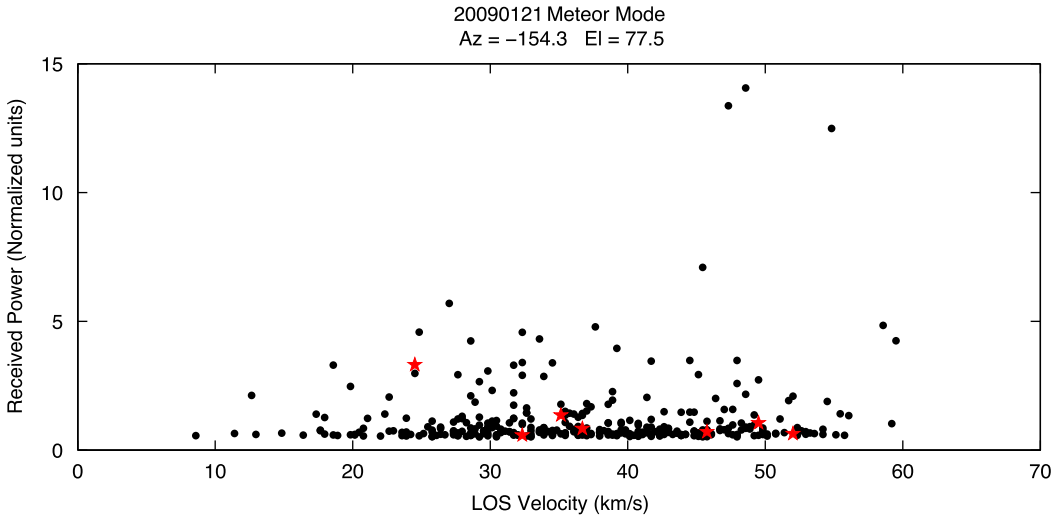

Fig. 5. Scatter plot showing the backscattered power versus the LOS velocity of each meteor. The black dots show the meteors detected in the radar data and the red stars show the meteors visible in both the radar and imager data.

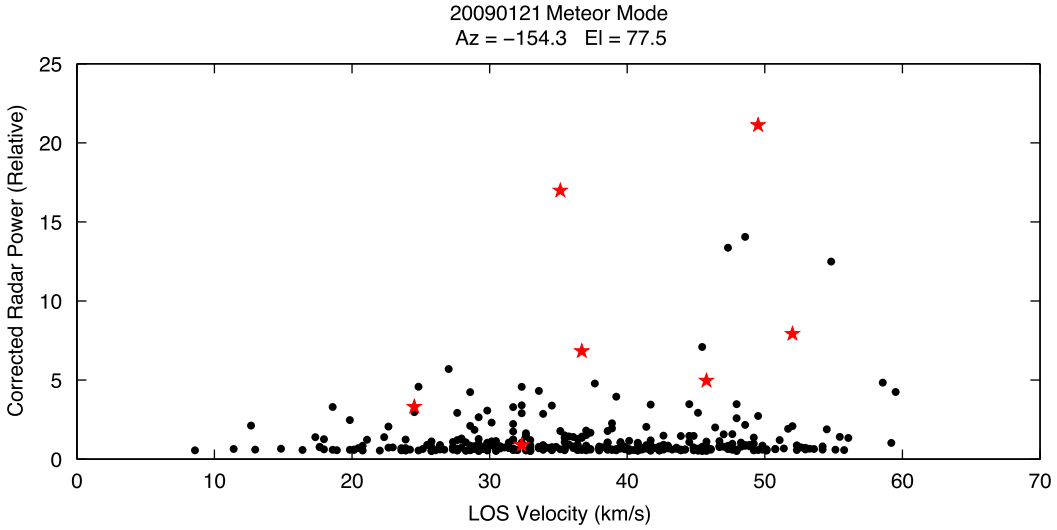

Fig. 6. Scatter plot showing the corrected backscattered power versus the LOS velocity of each meteor. The black dots show the meteors detected in the radar data and the red stars show the meteors visible in both the radar and imager data.

known attenuation and locations of the side lobes. This correction was also checked against the power received in other beams when some of these meteors passed directly through them. Fig. 6 shows the same data as Fig. 5 but in this case, the radar power has been corrected for the seven optical meteors. There does appear to be a correlation between the backscattered power and the LOS velocity for the optical meteors, with the higher velocities corresponding to larger backscattered power. This is consistent with theory, as faster meteors should produce greater ionization. The increased production of free electrons could results in a larger scattering cross-section (Close et al., 2007; Janches et al., 2008), although it has been shown that the actual distribution of electrons plays a significant role in determining the radar scattering cross-section (Mathews, 2004).

Fig. 7 shows a scatter plot of the optical brightness versus the corrected radar power. The solid line is a linear fit showing that there is a correlation between backscattered power and optical brightness, with brighter meteors corresponding to larger backscattered power. The relationship between optical brightness and radar power is not as simple as Fig. 7 implies.

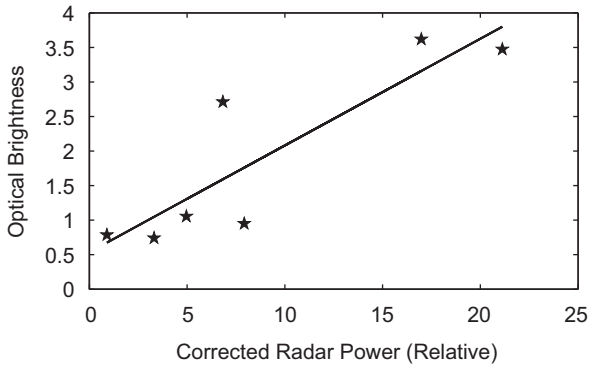

Fig. 7. Scatter plot of the optical brightness versus the corrected radar power for each meteor. The solid line is a linear fit to the data.

There are many complexities that need to be taken into account, for example the effects of meteor fragmentation on the backscattered power (Verniani, 1969; Mathews et al.,

2010). In fact, Fig. 7 is meant to show the potential usefulness of combining radar with optics for meteor science, and given the unaccounted for complexities, it cannot be used to derive any quantitative correlation.

The imager FOV was centered along the direction of the radar beam (close to vertical), so the imager shows the perpendicular (to the radar beam) projection of the meteor's velocity. Therefore, the combination of the radar LOS velocity with the perpendicular speed and direction from the images gives the complete velocity vector. The magnitude of the velocity vector can be computed and will be referred to as the absolute meteor speed. The wealth of information obtained from both the optics and the radar enables the comparison of many different quantities and Fig. 8 shows a series of scatter plots of these: (a) absolute meteor speed versus received radar power, (b) absolute meteor speed versus relative optical brightness, (c) origin direction (0° is north, 90° is east) versus received radar power, and (d) origin direction versus relative optical brightness. There are similarities between the radar power plots on the left and the optical intensity plots on the right. Both show a correlation with the absolute meteor speed, faster meteors correspond to higher intensity. In addition, the meteors that originate in the east are more intense in the radar and optically which is consistent with faster velocities from the easterly direction.

Measuring both the horizontal and vertical component of velocity allows for the calculation of the angle of incidence into the atmosphere. Fig. 9 shows (a) the scatter plot of the incidence angle, (0° is straight in), versus origin direction (0° is north, 90° is east) and (b) the absolute speed of each meteor versus its origin direction. This shows that the meteors originating in the east (90°) have a higher angle of incidence than those originating in other directions. It appears that there may be a minimum in the incidence angle for meteors coming from the north. The incidence angle is dependent on local effects, such as latitude, season and local time, so observations from this limited case study are not useful in determining the sources of meteors. However, when combined with the origin direction and with a more complete statistical sampling of data from PFISR over different local times and seasons, the observed meteors can be assigned to their respective apparent radiant locations.

There are errors in the method of estimating the perpendicular speed of the meteor from the optical images. The image data allow a horizontal projection of the meteors speed to be measured over a relatively short path of 5–20 km, where the meteors ablate and produce enough light to be detected. In addition, the luminous portion of the meteors trajectory may not actually coincide with the radar beam (or side lobe) location, which leads to errors in the velocity measurements. The largest source of

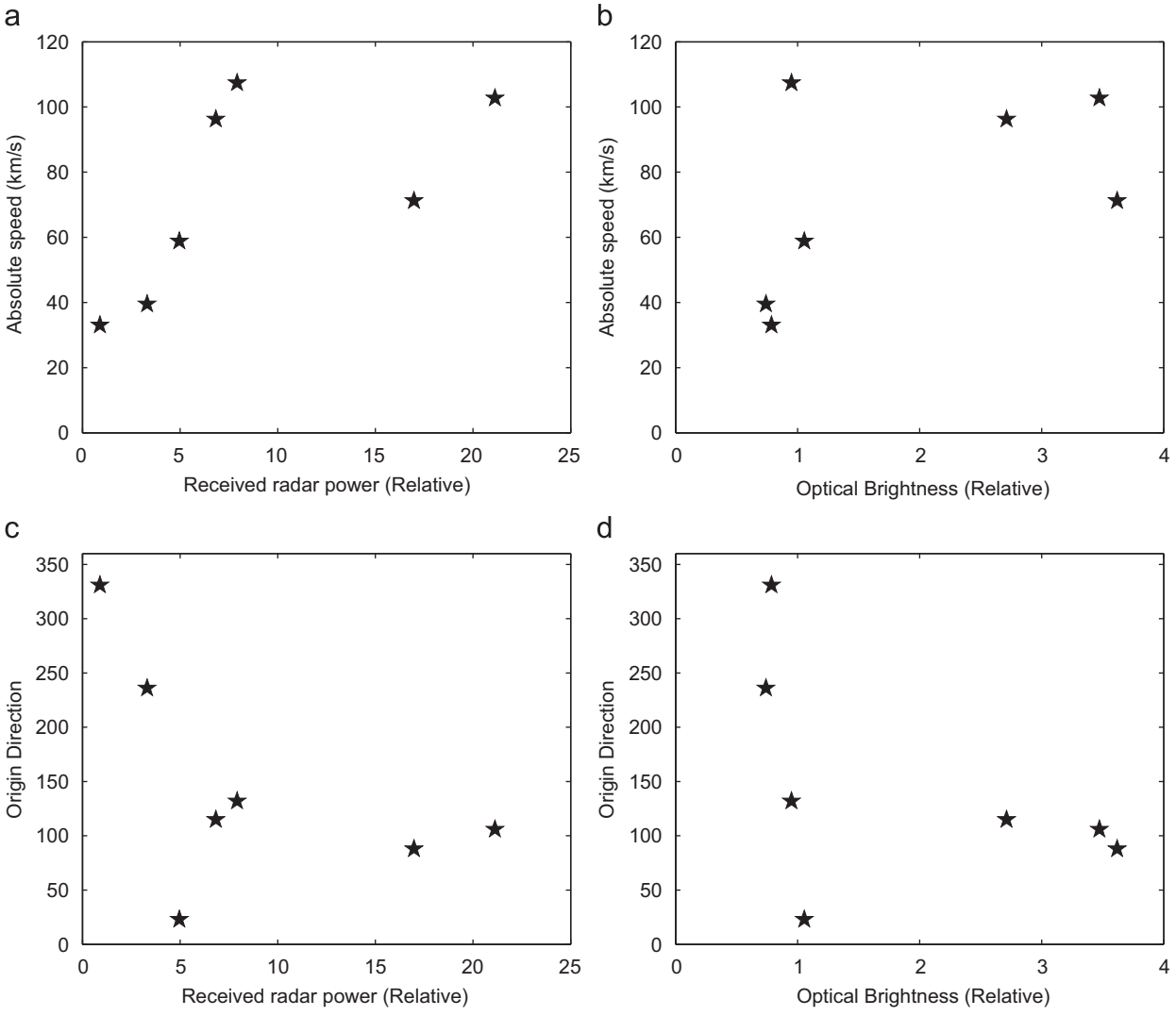

Fig. 8. Scatter plots showing the (a) absolute meteor speed versus radar power, (b) absolute meteor speed versus optical brightness, (c) origin direction versus radar power, and (d) origin direction versus optical brightness.

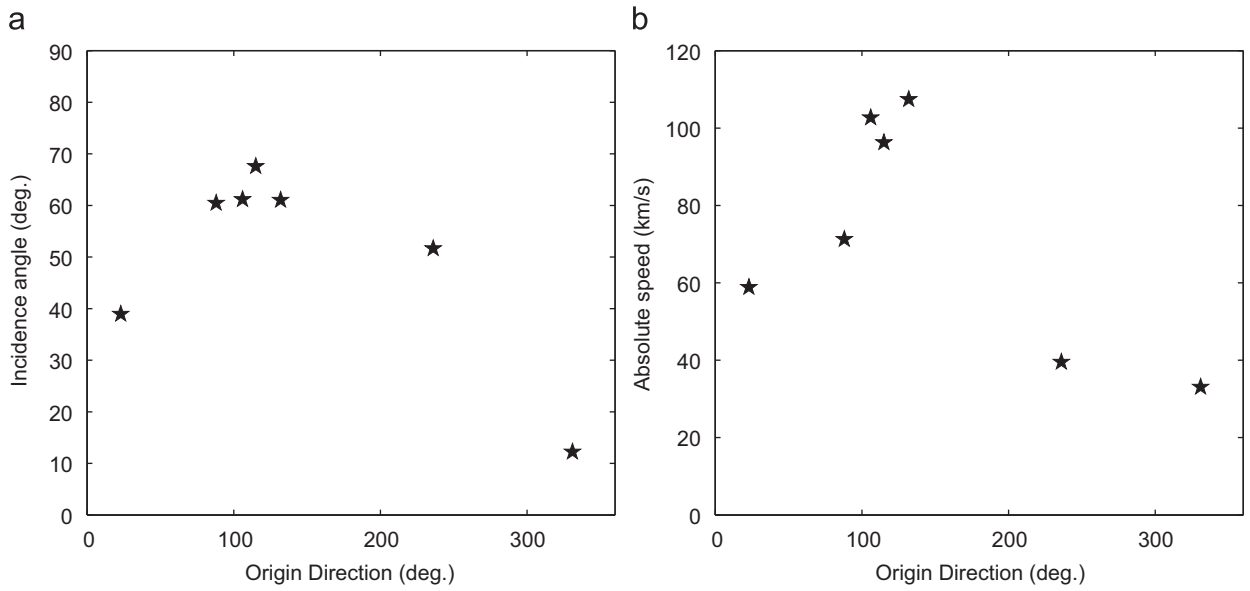

Fig. 9. Scatter plots showing (a) the incidence angle (0° is straight in) into the atmosphere versus the origin direction (0° is north, 90° is east) for each meteor and (b) the absolute speed of each meteor versus its origin direction.

velocity errors in these measurements comes from aspect angle effects, as the imagers and radar are not centered on the zenith, but rather 13° off. This potentially leads to errors of up to 20% in the speeds measured by both methods because some component of the absolute meteor velocity could be detected in both the radar and the imager, and the analysis here assumed that the two measured components were independent. The absolute meteor speeds presented here could therefore be overestimates, based on the known sources of error. There is interest in measuring meteors with absolute velocities over 72 km/s, which could be of extra solar origin; however, no convincing measurements have been made (Meisel et al., 2002a,b). A carefully constructed experiment of this type (combining high-resolution optics with radars) could be used to accurately measure both components of the meteor's velocity, specifically targeting the detection of high velocity (>72 km/s) meteors.

The main source of meteor input to Earth's atmosphere is from the Sporadic Meteor Complex (SMC), which is composed of six radiant distributions. These are the North Apex, South Apex, Helion, Antihelion, North Toroidal and South Toroidal (Jones and Brown, 1993; Taylor, 1997; Taylor and Elford, 1998). Fentzke et al. (2009) modeled the expected meteor flux at PFISR from each of these sources, which can be compared to observations when the radiant locations of meteors are determined from the combined radar and optical observations.

3. Discussion

Although there are limitations to the interpretation of only seven data points, there are several significant observations.

First, optically visible meteors are observed in the PFISR data. They are even observable in the 2006 ion line mode data, when the receiver was set to filter out such high Doppler shift returns. The detailed analysis of the 2009 meteor mode data, examined in this case study, found that during a four hour period there were a total of 338 meteors detected with the radar and seven of those were visible in the optical data. This reveals that only about 2% of the radar meteors are visible optically, indicating that most of the meteors are too small to produce visible trails. However, the open question is whether the properties of the non-optical meteors can be extrapolated from those that are observed with both optics and radar. For example, can the mass estimates derived from the optical data be used to infer the masses of the meteors that are only observed with the radar? Sparks et al. (2009) reported the average masses of meteors, derived from PFISR data, for different seasons. They reported an average mass of 0.0024 μg for winter observations, which is much less than the expected limit of 10 μg for producing visible trails (Rogers et al., 2004). Therefore it is expected that only a small fraction of the total radar meteors should be associated with optical trails.

Another important observation made possible by the combination of imager and PFISR data, is that a large fraction of the meteors actually occurred in side lobes and not within the main beam of the radar. For the case of the optical meteors, 6 out of the 7, or about 85% were observed in the side lobes. This could have serious implications for studies, using only radar data, that are examining and quantifying the backscattered power of meteors. Without knowing where the meteor occurred relative to the main beam, the values obtained for the backscattered power could be off by an order of magnitude or more. For example, a weak backscattered signal could have resulted from a small meteor in the main beam, which is typically assumed, or from a large meteor in a far side lobe, which might actually occur more frequently. This observation is inconsistent with the results reported in Chau et al. (2009), where they found, using an antenna compression approach, that more than 15% of the total meteors observed with PFISR occurred in the side lobes. One possible explanation for this discrepancy is that the analysis presented here assumed that the properties of the optical meteors could be extrapolated to the PFISR meteors, but this may not be true for the smaller meteors. The optical meteors produce a large cloud of electrons which can very effectively scatter the radar signal, therefore the scattering cross-section will be large enough to be detected by the side lobes. On the other hand the small (non-optical) meteors may not produce enough cross-section to be detected with the side lobes. This would effectively produce a selection effect, where all the optical meteors are by definition large enough to be detected by any of the side lobes, while the small ones are not. In order to address this issue, the connection between scattering cross-section, mass, and optical luminosity needs to be determined in statistically significant detail, for which

this paper is meant to show is possible given a larger number of observations.

The backscattered power contained within the meteor return is used to calculate the radar scattering cross-section of the meteor. This is assumed to be a direct relationship; more power equals larger scattering cross-section. Again, the assumption is that the meteors are all within the main beam. There have been recent efforts to model and estimate meteoroid mass based on the radar scattering and predicted optical intensities (Close et al., 2005; Rogers et al., 2004; Dyrud and Janches, 2008). The optical intensity can be used as a proxy for meteoroid mass, the brighter trails resulting from bigger meteoroids. Since far more meteors are observed with radars than with optical methods, it would be advantageous to have a way to accurately estimate meteor mass from the radar data alone. In order to do so, one first needs to understand the relationship between the radar scattering cross-section and the optical brightness which should, in theory, provide a direct measure of the mass. Fig. 7 shows this relationship for the seven optically observed meteors, demonstrating that there is a correlation between the corrected backscattered power and the optical brightness. However, this relationship only holds for the actual scattering cross-section of the meteor, not the apparent one if the meteor occurred in a side lobe.

The correlations among the remaining quantities obtained seem consistent with currently held notions about meteors. Faster meteors tend to produce brighter signals both optically and in the radar data. They also tend to come from the east, consistent with the motion of the Earth and therefore producing brighter signals in the optical and radar data.

Lastly, this type of observation could have implications in determining the origin of the meteoroid material. For example, Fig. 9a shows the relationship between the origin direction and the incidence angle into the atmosphere. The origin direction reveals where, in the ecliptic plane, the meteoroids are coming from, and the incidence angle contains information about the component of velocity perpendicular to the ecliptic plane, given the high latitude location of Poker Flat. Fig. 9b demonstrates the relationship between the absolute speed and origin direction. These observations are meant to demonstrate that this method can be used to compute the incidence angle and origin direction of meteors. This information can then be used to determine the apparent radiant location of each meteor in heliocentric coordinates (right ascension and declination). This would enable their assignment to the six sectors of the SMC or to specific meteor showers.

4. Conclusion

The 2006 PFISR data revealed that optical meteors could be observed by PFISR, even when the radar mode was non-optimal for meteor Doppler shifts; however, quantitative comparisons could not be done with those data.

In order to make such comparisons, a meteor mode was developed by SRI, where one receiver channel was set specifically to record at higher bandwidth for subsequent observational campaigns. During these campaigns, high-resolution imager data were recorded to capture any visible meteors that passed through the radar beam locations. The four hours of data recorded on 21 January 2009 provided a good initial case study to determine the extent to which the optical meteors were observed in the PFISR data and the usefulness of the data set for a statistical study.

Seven meteors were observed optically and all were detected by PFISR, which observed a total of 338 meteors. This reveals that only about 2% of the radar meteors are visible optically, indicating that most of them are too small to produce visible trails. It is also possible that some were detected by far side lobes of the radar and produced visible trails outside the FOV of the imager. Of the seven optical meteors, only one passed directly through the main beam of the radar, while the other six were detected in side lobes. Therefore only about 15% of the optical meteors detected with the radar are actually in the main beam. Assuming that smaller meteors produce enough radar cross-section to be detected by the side lobes, the backscattered power measurements could be wrong for about 85% of detected meteors. Although this may not be true for all meteors, it is certainly true for some meteors and therefore this relationship needs to be more fully understood. A sample size of only seven meteors results in error bars of 40%. In order to reduce that to approximately 5%, for statistical significance, a sample size of 400 is needed. This is a feasible task, given the data already on hand (estimated to contain approximately 200 optical meteors) and from upcoming campaigns.

Assuming that backscattered power from meteors, corrected for side lobe attenuation, can be used as a proxy for radar scattering cross-section and that optical brightness can be used as a proxy for meteoroid mass, it was found that there is a positive correlation between the scattering cross-section and mass of meteors. The optically brighter (also faster) meteors produce more radar backscatter.

It can be noted that the absolute speeds of some of the observed meteors are greater than the 72 km/s limit for hyperbolic heliocentric orbits, indicating that they are on hyperbolic orbits (Hill et al., 2005; Rogers et al., 2004). The large proportion of high velocity meteors observed optically is likely due to a selection effect. For a meteoroid of a given mass, there is a direct relationship between speed and ionization (faster speed implies more ionization). Greater ionization leads to a greater probability of producing a visible trail.

The combination of the radar and optical data allows for the unique velocity vector (origin direction, incidence angle and absolute speed) of each meteor to be determined. Meteors originating in the east have higher speeds and more glancing incidence angles, while meteors originating in the north have lower speeds and more direct incidence angles. These relationships can be used to determine the apparent radiant location of each meteor in heliocentric coordinates, allowing assignment to the known radiant sources.

This study shows that optical meteors are observed by PFISR and indicates the trends to be expected. The seven data points provide a good first look at what kind of relationships can be determined from combining optical and radar observational techniques for meteor studies. The next step is to continue these analyses with many additional observations in order to improve the statistics.

Acknowledgments

This work was supported by National Science Foundation Grant # ATM-0836410. The author would like to thank SRI International, and specifically C. Heinselman for many useful discussions, as well as arranging the meteor mode and coordinating PFISR time. Thanks also to The University of Alaska, Fairbanks/Geophysical Institute for the use of their facilities and imagers at Poker Flat, AK, particularly H.C. Stenbaek-Nielsen and D. Hampton. The author is indebted to M. Samara for assistance in data collection and manuscript editing.

References

Appleton, E., Naismith, R., 1947. The radio detection of meteor trails and allied phenomena. Proc. Phys. Soc. 59 (May), 461–473.

Bakharev, A.M., Mukhamednazarov, S., Shodiev, U., 1977. Photometry of television spectra of meteor trails. Astron. Vestn. 11 (March), 60–63.
Briczinski, S.J., Mathews, J.D., Meisel, D.D., 2009. Statistical and fragmentation properties of the micrometeoroid flux observed at Arecibo. J. Geophys. Res. 114 (April), 4311.
Brosch, N., Polishook, D., Helled, R., Schijvarg, S., Rosenkrantz, M., 2004. Radar and optical leonids. Atmos. Chem. Phys. 4 (July), 1063–1069.
Chau, J.L., Galindo, F.R., Heinselman, C.J., Nicolls, M.J., 2009. Meteor-head echo observations using an antenna compression approach with the 450 MHz Poker Flat Incoherent Scatter Radar. J. Atmos. Sol. Terr. Phys. 71 (May), 636–643.
Clemesha, B.R., de Medeiros, A.F., Gobbi, D., Takahashi, H., Batista, P.P., Taylor, M.J., 2001. Multiple wavelength optical observations of a long-lived meteor trail. Geophys. Res. Lett. 28 (July), 2779–2782.
Close, S., Brown, P., Campbell-Brown, M., Oppenheim, M., Colestock, P., 2007. Meteor head echo radar data: mass velocity selection effects. Icarus 186 (February), 547–556.
Close, S., Oppenheim, M., Durand, D., Dyrud, L., 2005. A new method for determining meteoroid mass from head echo data. J. Geophys. Res. 110 (September), 9308.
Close, S., Oppenheim, M., Hunt, S., Dyrud, L., 2002. Scattering characteristics of high-resolution meteor head echoes detected at multiple frequencies. J. Geophys. Res. 107 (October), 1295.
Dyrud, L., Janches, D., 2008. Modeling the meteor head echo using Arecibo radar observations. J. Atmos. Sol. Terr. Phys. 70 (September), 1621–1632.
Dyrud, L.P., Kudeki, E., Oppenheim, M., 2007. Modeling long duration meteor trails. J. Geophys. Res. 112 (December), 12307.
Dyrud, L.P., Oppenheim, M.M., Close, S., Hunt, S., 2002. Interpretation of non-specular radar meteor trails. Geophys. Res. Lett. 29 (21), 2012.
Fentzke, J.T., Janches, D., Sparks, J.J., 2009. Latitudinal and seasonal variability of the micrometeor input function: a study using model predictions and observations from Arecibo and PFISR. J. Atmos. Sol. Terr. Phys. 71 (May), 653–661.
Fujiwara, Y., Ueda, M., Nakamura, T., Tsutsumi, M., 1995. Simultaneous observations of meteors with the radar and TV systems. Earth Moon Planets 68 (January), 277–282.
Grime, B.W., Kane, T.J., Collins, S.C., Kelley, M.C., Kruschwitz, C.A., Friedman, J.S., Tepley, C.A., 1999. Meteor trail advection and dispersion; preliminary lidar observations. Geophys. Res. Lett. 26 (March), 675–678.
Hapgood, M.A., Rothwell, P., 1982. Structure of small meteoroids deduced from two station low light level TV observations of meteor trails. In: The comparative study of the planets, pp. 311–315.
Hill, K.A., Rogers, L.A., Hawkes, R.L., 2005. High geocentric velocity meteor ablation. Astron. Astrophys. 444 (December), 615–624.
Janches, D., Close, S., Fentzke, J.T., 2008. A comparison of detection sensitivity between ALTAIR and Arecibo meteor observations: can high power and large aperture radars detect low velocity meteor head-echoes. Icarus 193 (January), 105–111.
Janches, D., Nolan, M.C., Meisel, D.D., Mathews, J.D., Zhou, Q.H., Moser, D.E., 2003. On the geocentric micrometeor velocity distribution. J. Geophys. Res. 108 (June), 1222.
Jones, J., Brown, P., 1993. Sporadic meteor radiant distributions—orbital survey results. Mon. Not. R. Astron. Soc. 265 (December), 524.
Kaiser, N., Brown, P., Hawkes, R.L., 2004. Optical trail width measurements of faint meteors. Earth Moon Planets 95 (December), 579–586.
Lovell, A.C.B., Clegg, J.A., 1948. Characteristics of radio echoes from meteor trails: I. The intensity of the radio reflections and electron density in the trails. Proc. Phys. Soc. 60 (May), 491–498.
Mathews, J.D., 2004. Radio science issues surrounding HF/VHF/UHF radar meteor studies. J. Atmos. Sol. Terr. Phys. 66 (February), 285–299.
Mathews, J.D., Briczinski, S.J., Malhotra, A., Cross, J., 2010. Extensive meteoroid fragmentation in V/UHF radar meteor observations at Arecibo observatory. Geophys. Res. Lett. 37 (February), 4103.
Mathews, J.D., Briczinski, S.J., Meisel, D.D., Heinselman, C.J., 2008. Radio and meteor science outcomes from comparisons of meteor radar observations at AMISR Poker Flat, Sondrestrom, and Arecibo. Earth Moon Planets 102 (June), 365–372.
Mathews, J.D., Doherty, J., Wen, C., Briczinski, S.J., Janches, D., Meisel, D.D., 2003. An update on UHF radar meteor observations and associated signal processing techniques at Arecibo observatory. J. Atmos. Sol. Terr. Phys. 65 (July), 1139–1149.
McNeil, W., 1999. Modeling of meteor trails as observed by LIDAR. In: Jenniskens, P. (Ed.), The Leonid MAC Workshop, NASA Ames Research Center, CA, April 12–15, 1999, Meteoritics & Planetary Science, Meeting Abstract.
Meisel, D.D., Janches, D., Mathews, J.D., 2002a. Extrasolar micrometeors radiating from the vicinity of the local interstellar bubble. Astrophys. J. 567 (March), 323–341.
Meisel, D.D., Janches, D., Mathews, J.D., 2002b. The size distribution of Arecibo interstellar particles and its implications. Astrophys. J. 579 (November), 895–904.
Oppenheim, M.M., Dyrud, L.P., vom Endt, A.F., 2003. Plasma instabilities in meteor trails: 2-D simulation studies. J. Geophys. Res. 108 (February), 1064.
Oppenheim, M.M., vom Endt, A.F., Dyrud, L.P., 2000. Electrodynamics of meteor trail evolution in the equatorial E-region ionosphere. Geophys. Res. Lett. 27 (October), 3173–3176.
Pellinen-Wannberg, A., Westman, A., Wannberg, G., Kaila, K., 1998. Meteor fluxes and visual magnitudes from EISCAT radar event rates: a comparison with cross-section based magnitude estimates and optical data. Ann. Geophys. 16 (November), 1475–1485.
Reddi, C.R., Nair, S.M., 1998. Meteor trail induced backscatter in MST radar echoes. Geophys. Res. Lett. 25, 473–476.
Rogers, L.A., Hill, K.A., Hawkes, R.L., 2004. Optical predictions for high geocentric velocity meteors. Earth Moon Planets 95 (December), 237–244.
Shamir, L., 2005. Analysis of meteor trails using the Night Sky Live network of panoramic CCD cameras. WGN, J. Int. Meteor Org. 33 (June), 75–80.
Sparks, J.J., Janches, D., Nicolls, M.J., Heinselman, C.J., 2009. Seasonal and diurnal variability of the meteor flux at high latitudes observed using PFISR. J. Atmos. Sol. Terr. Phys. 71 (May), 644–652.
Szasz, C., Kero, J., Pellinen-Wannberg, A., Meisel, D.D., Wannberg, G., Westman, A., 2008. Estimated visual magnitudes of the EISCAT UHF meteors. Earth Moon Planets 102 (June), 373–378.
Taylor, A.D., 1997. Radiant distribution of meteoroids encountering the earth. Adv. Space Res. 20, 1505–1508.
Taylor, A.D., Elford, W.G., 1998. Meteoroid orbital element distributions at 1 AU deduced from the Harvard Radio Meteor Project observations. Earth Planets Space 50 (June), 569–575.
Verniani, F., 1969. Structure and fragmentation of meteoroids. Space Sci. Rev. 10 (November), 230–261.
Von Zahn, U., 1999. Meteor trail observations during the Leonids 1996 and 1998 by groundbased lidar(s) and co-located CCD camera. In: Jenniskens, P. (Ed.), The Leonid MAC Workshop, NASA Ames Research Center, CA, April 12–15, 1999, Meteoritics & Planetary Science, Meeting Abstract.
Von Zahn, U., 2001. Lidar observations of meteor trails: evidence for fragmentation of meteoroids and their subsequent differential ablation. In: Warmbein, B. (Ed.), Meteoroids 2001 Conference, vol. 495. ESA Special Publication, pp. 303–314 November.
Znojil, V., Grygar, J., Mikulasek, Z., Simek, M., Sulc, M., 1980. The relation between meteor optical brightness and properties of the ionized trail. I—observational techniques and basic characteristics of the observational data/results of the meteor expeditions Ondrejov 1972 and 1973/. Bull. Astron. Inst. Czech. 31, 14–25.